Plan B for particle physics: finding long lived particles at CERN

Bondarenko, K.

Author: Bondarenko, K.
Title: Plan B for particle physics: finding long lived particles at CERN
Issue Date: 2018-11-15

Chapter 3

Neutrino portal

In general, the number of model parameters in the neutrino portal increases with the number of HNLs (see e.g. reviews [144, 210]). For example, the model containing two sterile neutrinos has a total of eleven free parameters, whereas the model with three has a total of eighteen free parameters [144]. Despite this, not all of them play an important role, since phenomenology is sensitive to only the mass of the HNL(s) and the absolute values of mixing angles, $|U_{\alpha I}|$.

In contrast to the behavior of active neutrinos, sterile neutrinos that are no degenerate in mass are produced and decay independently – i.e., without oscillations between themselves. Thus, from a phenomenological point of view it is sufficient to describe one sterile neutrino with only four parameters: the sterile neutrino mass M_N plus the mixing angles with the three known active neutrinos U_α, see Eq. (1.5.2) for fixed I value. Such *Heavy Neutral Leptons* can be searched for in different high-energy experiments. In this section, we will discuss their phenomenology.

3.1 HNL production in proton fixed-target experiments

In fixed-target experiments, such as NA62, SHiP or DUNE, the initial interaction is a proton-nuclei collision. In such collisions, HNLs can be produced in a number of ways:

a) Production from hadron decays;
b) Production from Deep Inelastic Scattering (DIS) p-nucleon interaction;
c) Production from the coherent proton-nucleus scattering.

Below we provide an overview of each of the channels summarizing previous results and emphasizing novel points.

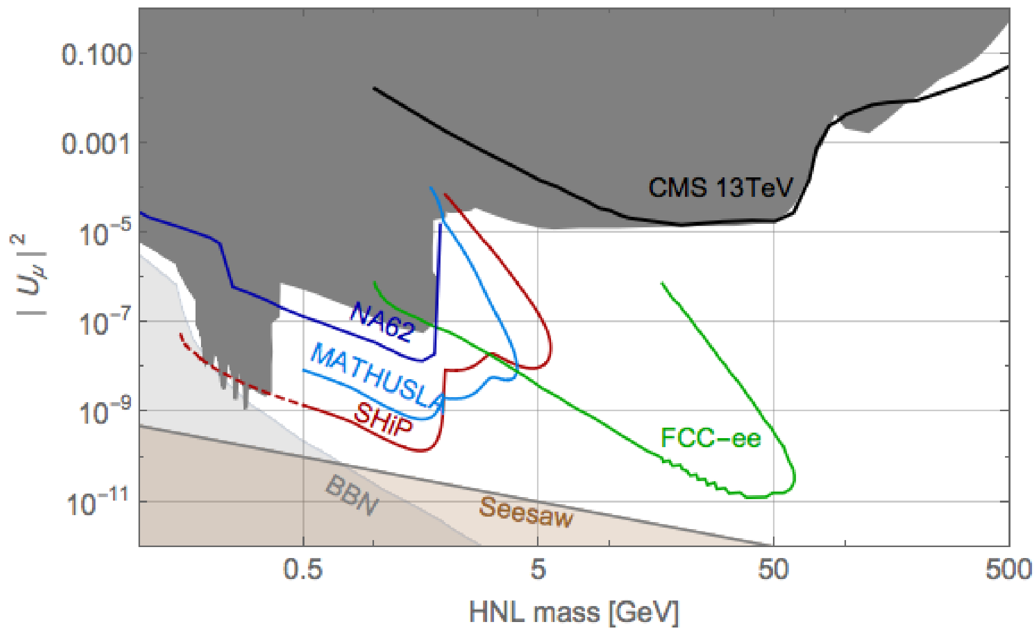

Figure 3.1: Existing limits and future prospects for searches for HNLs. Only mixing with muon flavor is shown. For the list of previous experiments (gray area) see [110]. The black solid line is a recent bound from the CMS 13 TeV run [211]. The sensitivity estimates from prospective experiments are based on [168] (FCC-ee), [109] (NA62), [212] (SHiP) and [213] (MATHUSLA). The sensitivity of SHiP below kaon mass (dashed line) is based on the number of HNLs produced in the decay of D-mesons only and does not take into account contributions from kaon decays, see [212] for details. The primordial nucleosynthesis bounds on HNL lifetime are from [214]. The Seesaw line indicates the parameters obeying the seesaw relation $|U_\mu|^2 \sim m_\nu/M_N$, where for active neutrino mass we substitute $m_\nu = \sqrt{\Delta m^2_{\text{atm}}} \approx 0.05\,\text{eV}$ [110].

3.1.1 Production from hadrons

The main channels of HNL production from hadrons are via decays of sufficiently long-lived hadrons, i.e. the lightest hadrons of each flavor[1]. In the framework of the Fermi theory, the decays are inferred by the weak charged currents. One can also investigate the production through neutral current from the hidden flavored mesons $J/\psi(c\bar{c}, 3097)$, $\Upsilon(b\bar{b}, 9460)$ as sources of HNLs. These mesons are short-lived, but 1.5–2 times heavier than the corresponding open flavored mesons, giving a chance to produce heavier HNLs.

Since the region of HNL masses below that of the kaon is strongly constrained by previous experiments (see [110] for details, reproduced in Fig. 3.1), we concentrate on the production channels for HNL masses $M_N > 0.5$GeV.

[1]Such hadrons decay *only* through weak interactions with relatively small decay width (as compared to electromagnetic or strong interaction). As the probability of HNL production from the hadron's decay is inversely proportional to the hadron's decay width, the HNL production from the lightest hadrons is significantly more efficient.

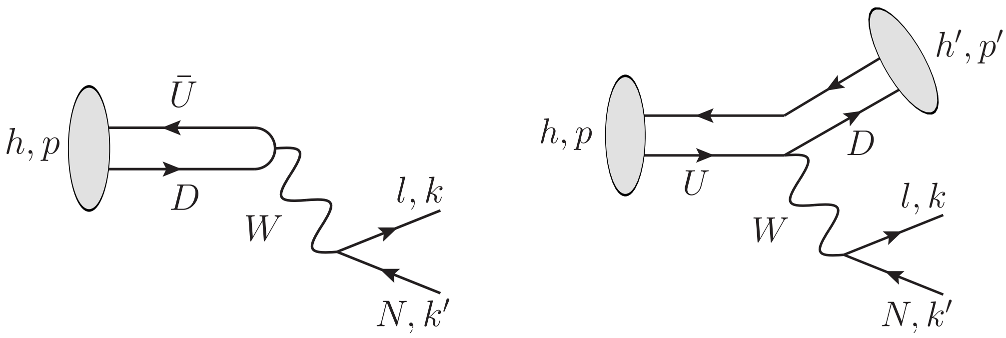

Figure 3.2: *Left:* The diagram of leptonic decay of the meson h with 4-momentum p. *Right:* The diagram of semileptonic decay of the meson h with 4-momentum p into meson h' with 4-momentum p'. In both diagrams the 4-momentum transferred to the lepton pair is $q = k + k'$.

HNLs are produced in meson decay either via a 2-body purely leptonic decay (left panel of Fig. 3.2) or semileptonic decay (right panel of Fig. 3.2) [215, 216]. The branching fractions of the leptonic decay have already been determined e.g. in [217, 218]. However, in the case of semileptonic decays, only the processes with a single pseudo-scalar or vector meson in the final state have been considered so far [218] (see also [219] and [220])

$$h \to h'_P \ell N \tag{3.1.1}$$
$$h \to h'_V \ell N \tag{3.1.2}$$

(where h'_P is a *pseudo-scalar* and h'_V is a *vector* meson). We reproduce computations of the branching ratios for these production channels in the Appendix A paying special attention to the treatment of form factors.

Finally, to calculate the number of produced HNLs one should ultimately know the *production fraction*, $f(\bar{q}q \to h)$ i.e. the probability a given hadron being produced from the corresponding heavy quark. It can either be determined experimentally or computed from Pythia simulations (as e.g. in [221]).

3.1.1.1 Production from light unflavored and strange mesons

Among the light unflavored and strange mesons the relevant mesons for the HNL production are:[2] $\pi^+(u\bar{d}, 139.6)$, $K^+(u\bar{s}, 494)$, $K^0_S(d\bar{s}, 498)$ and $K^0_L(d\bar{s}, 498)$.

The only possible production channel from the π^+ is the 2-body decay $\pi^+ \to \ell^+_\alpha N$ with $\ell = e, \mu$. The production from K^+ is possible through the 2-body decay of the same type. There are also 3-body decays $K^+ \to \pi^0 \ell^+_\alpha N$ and $K^0_{L/S} \to \pi^- \ell^+_\alpha N$.

[2] The particle lists here and below are given in the format 'Meson name(quark contents, mass in MeV)').

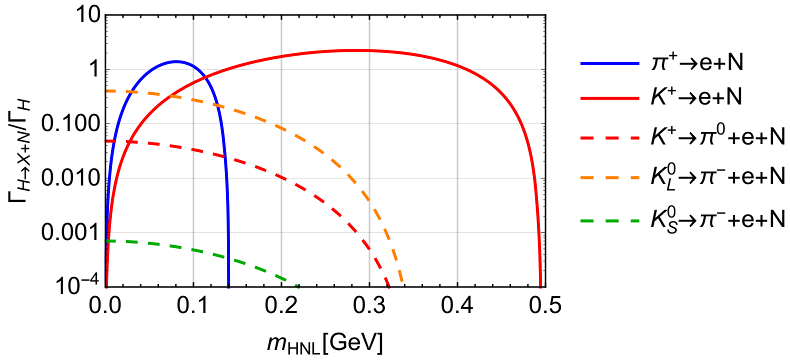

Figure 3.3: Decay width to HNLs divided by the measured total decay width for pions and kaons correspondingly. In this Figure we take $U_e = 1$, $U_\mu = U_\tau = 0$.

The resulting branching ratios for corresponding mesons are shown in Fig. 3.3. For small HNL masses, the largest branching ratio is that of $K_L^0 \to \pi^- \ell_\alpha^+ N$ due to the helicity suppression in the 2-body decays and small decay width of K_L^0.

3.1.1.2 Production from charmed mesons

The following charmed mesons are most relevant for the HNL production: $D^0(c\bar{u}, 1865)$, $D^+(c\bar{d}, 1870)$, $D_s(c\bar{s}, 1968)$.

D^0 is a neutral meson and therefore its decay through the charged current interaction necessarily involves a meson in a final state. The largest branching is to K meson, owing to the CKM suppression $|V_{cd}|/|V_{cs}| \approx 0.22$. Then the mass of the resulting HNL is limited to $M_N < M_D - M_K \approx 1.4$GeV. For the charmed *baryons* the same argument is applicable: they should decay into baryons and the most probable is strange baryon, hence $M_N < M_{\Lambda_c} - M_\Lambda \approx 1.2$GeV. Therefore these channels are open only for HNL mass *below* ~ 1.4GeV.

Charged charmed mesons $D^\pm$ and D_s would exhibit 2-body decays into an HNL and a charged lepton, so they can produce HNLs almost as heavy as themselves. The branching ratio of $D_s \to N + X$ is more than 10 times larger than any ratio of other D-mesons. The number of D_s mesons is, of course, suppressed as compared to $D^\pm$ and D^0 mesons, however only by a factor of few[3]. Indeed, at energies relevant for $\bar{c}c$ production, the fraction of strange quarks is already sizeable, $\chi_{\bar{s}s} \sim 1/7$ [222]. *As a result, the two-body decays of D_s mesons dominate in the HNL production from charmed mesons*, see Fig. 3.4.

3.1.1.3 Production from beauty mesons

The lightest beauty mesons are $B^-(b\bar{u}, 5279)$, $B^0(b\bar{d}, 5280)$, $B_s(b\bar{s}, 5367)$, $B_c(b\bar{c}, 6276)$. Similarly to the D^0 case, neutral B-mesons (B^0 and B_s) decay through a charged

[3] For example at SPS energy (400 GeV) the production fractions of the charmed mesons are given by $f(D^+) = 0.204$, $f(D^0) = 0.622$, $f(D_s) = 0.104$ [221].

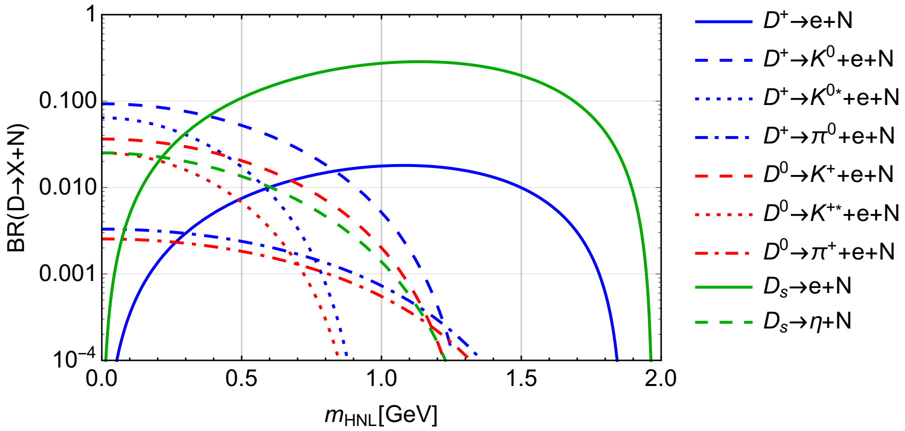

Figure 3.4: Dominant branching ratios of HNL production from different charmed and beauty mesons. For charged mesons 2-body leptonic decays are shown, while for the neutral mesons decays are necessarily semileptonic. For these plots we take $U_e = 1$, $U_\mu = U_\tau = 0$.

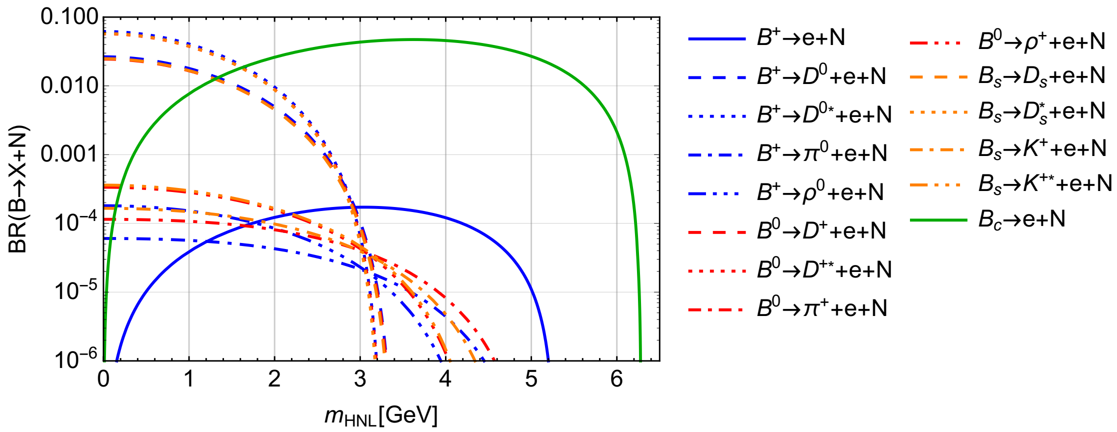

Figure 3.5: Dominant branching ratios of HNL production from different beauty mesons. For charged mesons 2-body leptonic decays are shown, while for the neutral mesons decays are necessarily semileptonic. For these plots we take $U_e = 1$, $U_\mu = U_\tau = 0$.

current with a meson in the final state. The largest branching is to the D meson because of the values of the CKM matrix elements ($|V_{cb}|/|V_{ub}| \approx 0.1$). Thus the mass of the resulting HNL is limited: $M_N < M_B - M_D \approx 3.4$ GeV.

Charged beauty mesons $B^\pm$ and $B_c^\pm$ have 2-body decays into HNL and charged lepton, so they can produce HNLs almost as heavy as themselves. Branching ratios of B-mesons into HNL for different decay channels and pure electron mixing are shown in Fig. 3.5.

The production fraction of $f(b \to B_c)$ has only been measured at LHC energies, where it is reaching a few $\times 10^{-3}$ [223]. At lower energies, it is not known. Nevertheless, production from B_c meson is an important production channel in the mass

Decay $B^+ \to \ell^+ \nu_\ell X$		BR [%]
Inclusive branching: $l = e,\ \mu$		11.0 ± 0.3
Dominant 1-meson channels: pseudo-scalar meson	$\overline{D}^0 \ell^+ \nu_\ell$	2.27 ± 0.11
vector meson	$\overline{D}^*(2007)^0 \ell^+ \nu_\ell$	5.7 ± 0.19
Two above channels together:		8.0 ± 0.2
Channels with 2 mesons:	$D^- \pi^+ \ell^+ \nu_\ell$	0.42 ± 0.05
	$D^{*-} \pi^+ \ell^+ \nu_\ell$	0.61 ± 0.06
$D^- \pi^+ \ell^+ \nu_\ell$ above is saturated by 1-meson modes	$\overline{D}_0^*(2420)^0 \ell^+ \nu_\ell$	0.25 ± 0.05
	$\overline{D}_2^*(2460)^0 \ell^+ \nu_\ell$	0.15 ± 0.02
$D^{*-} \pi^+ \ell^+ \nu_\ell$ is augmented with 1-meson modes	$\overline{D}_1(2420)^0 \ell^+ \nu_\ell$	0.30 ± 0.02
	$\overline{D}_1'(2430)^0 \ell^+ \nu_\ell$	0.27 ± 0.06
	$\overline{D}_2^*(2460)^0 \ell^+ \nu_\ell$	0.1 ± 0.02
Hence 1-meson modes contribute additionally		1.09 ± 0.12
Sum of other multi-meson channels, $n > 1$:	$\overline{D}^{(*)} n\pi \ell^+ \nu_\ell$	0.84 ± 0.27
Inclusive branching: $l = \tau$		not known
Dominant 1-meson channels: pseudo-scalar meson	$\overline{D}^0 \tau^+ \nu_\tau$	0.77 ± 0.25
vector meson	$\overline{D}^*(2007)^0 \tau^+ \nu_\tau$	1.88 ± 0.20

Table 3.1: Experimentally measured branching ratios for the main semileptonic decay modes of the B^+ and B^0 meson [222]. Decays to pseudoscalar (D) and vector (D^*) mesons together constitute 73% (for B^+) and 69% (for B^0). Charmless channels are not shown because of their low contribution

range $m_N \gtrsim 3.4$ GeV.

To understand this result let us compare HNL production from B_c with production from 2-body B^+ decay. Decay widths for both cases are given by (see Eq. (A.1.4))

$$\mathrm{Br}(h \to \ell_\alpha N) \approx \frac{G_F^2 f_h^2 m_h m_N^2}{8\pi\Gamma_h} |V_h^{\mathrm{CKM}}|^2 |U_\alpha|^2 K(m_N/m_h), \tag{3.1.3}$$

where we take $m_N \gg m_\ell$ and K is a kinematic suppression. Neglecting kinematic factor, the ratio for the numbers of HNLs is

$$\frac{N_{\mathrm{HNL}}(B_c \to \ell N)}{N_{\mathrm{HNL}}(B^+ \to \ell N)} \approx \underbrace{\frac{f_{b\to B_c}}{f_{b\to B^+}}}_{\approx 0.008} \times \underbrace{\frac{\Gamma_{B^+}}{\Gamma_{B_c}}}_{\approx 0.3} \times \underbrace{\left(\frac{f_{B_c}}{f_{B^+}}\right)^2}_{\approx 5} \times \underbrace{\frac{m_{B_c}}{m_{B^+}}}_{\approx 1.2} \times \underbrace{\left(\frac{V_{cb}^{\mathrm{CKM}}}{V_{ub}^{\mathrm{CKM}}}\right)^2}_{\approx 100} \approx 1.44. \tag{3.1.4}$$

We see that small fragmentation fraction of B_c meson is compensated by the ratio of CKM elements and meson decay constants.

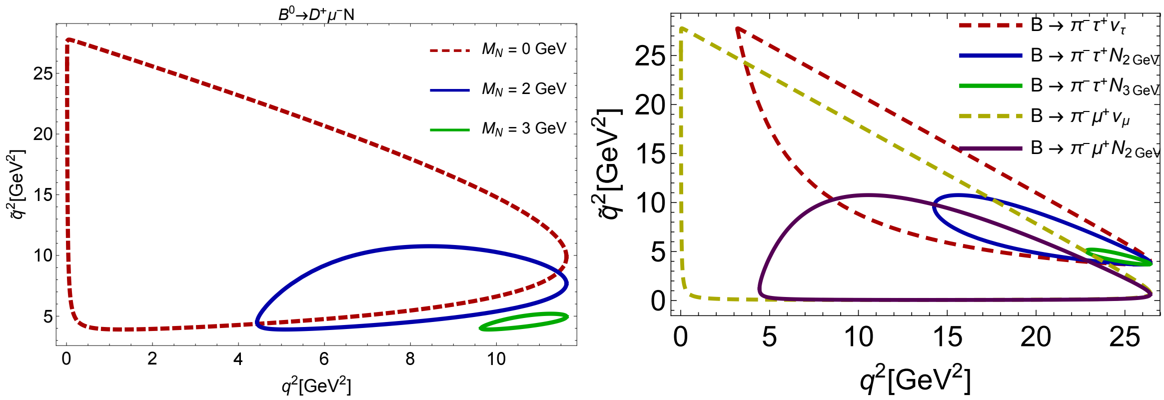

Figure 3.6: Dalitz plot for the semileptonic decay $B^0 \to D^+\mu^- N$. Available phase-space shrinks drastically when the HNL mass is large. q^2 is the invariant mass of the lepton pair, $\tilde{q}^2$ is the invariant mass of final meson and charged lepton.

3.1.1.4 Multi-hadron final states

D and especially B mesons are heavy enough to decay into HNL and multi-meson final states. While any single multi-meson channel would be clearly phase-space suppressed as compared to 2-body or 3-body decays considered above, one should check that the "inclusive" multi-hadron decay width does not give a sizeable contribution.

To estimate the relative relevance of single and multi-meson decay channels, we first consider the branching ratios of the semileptonic decays of B^+ and B^0 (with ordinary massless neutrino ν_ℓ in the final state)

$$B \to \ell^+ \nu_\ell X \quad , \quad l = e,\, \mu\,, \tag{3.1.5}$$

where X stands for one or many hadrons. The results are summarized in Table 3.1. Clearly, by taking into account *only* the single meson states we would *underestimate* the total inclusive width of the process (3.1.5) by about 20%.

In case of semileptonic decays with the HNL in the final state, the available phase-space shrinks considerably, see Fig. 3.6. The effect of the mass can also be estimated by comparing the decays involving light leptons (e/μ) to those with the τ-lepton in the final state. Comparison with SM decay rates into τ-lepton shows that 3-body decays into heavy sterile neutrinos are suppressed with respect to decays into light neutrinos. *Thus inclusive semileptonic decay of flavored mesons to HNLs are dominated by single-meson final states with the contributions from other states introducing a small correction.*

3.1.1.5 Quarkonia decays

Next we investigate the hidden flavored mesons $J/\psi(c\bar{c}, 3097)$ and $\Upsilon(b\bar{b}, 9460)$ as sources of HNLs. These mesons are short-lived, but 1.5-2 times heavier than the

Strange baryons	$\Lambda^0(uds, 1116)$, $\Sigma^+(uus, 1189)$, $\Sigma^-(dds, 1197)$, $\Xi^0(uss, 1315)$, $\Xi^-(dss, 1322)$, $\Omega^-(sss, 1672)$
Charmed baryons	$\Lambda_c(udc, 2287)$, $\Sigma_c^{++}(uuc, 2453)$, $\Sigma_c^0(ddc, 2453)$, $\Xi_c^+(usc, 2468)$, $\Xi_c^0(dsc, 2480)$, $\Omega_c^-(ssc, 2695)$, $\Xi_{cc}^+(dcc, 3519)$
Beauty baryons	$\Lambda_b(udb, 5619)$, $\Sigma_b^+(uub, 5811)$, $\Sigma_b^-(ddb, 5815)$, $\Xi_b^0(usb, 5792)$, $\Xi_b^-(dsb, 5795)$, $\Omega_b^-(ssb, 6071)$

Table 3.2: Long-lived flavored baryons. For each quark content (indicated in parentheses) only the lightest baryon of given quark content (ground state, masses are in MeV) is shown, see footnote 1 on page 42. The baryons considered in [221] have blue background. The baryons unobserved so far (such as $\Omega_{cc}^+(scc)$, $\Omega_{cb}(scb)$, etc.) are not listed.

corresponding open flavored mesons, giving a chance to produce heavier HNLs. We have studied these mesons in Appendix D, here we provide the summary of the results.

The number of HNLs produced from J/ψ decays is always subdominant to the number of HNLs produced in D-meson decays (for $M_N < m_D$). Therefore, the range of interest is $2\text{GeV} \leq M_N \leq m_{J/\psi}$ where this number should be compared with the number of HNLs produced via B-meson decays. The resulting ratio is given by

$$\frac{\text{HNLs from } J/\psi}{\text{HNLs from } B} = \frac{X_{c\bar{c}} \times f(J/\psi) \times \text{BR}_{J/\psi \to N\bar{\nu}}}{X_{b\bar{b}} \times f(B) \times \text{BR}_{B \to NX}} = \\ = 3 \times 10^{-4} \left(\frac{X_{c\bar{c}}}{10^{-3}}\right) \left(\frac{10^{-7}}{X_{b\bar{b}}}\right) \quad (3.1.6)$$

where we have adopted $f(B) \times BR(B \to N + X) \sim 10^{-2}$ (c.f. Fig. 3.5) and used $f(J/\psi) \sim 10^{-2}$. The numbers in (3.1.6) are normalized to the 400 GeV SPS proton beam. One sees that J/ψ can play a role only below $b\bar{b}$ production threshold (as $X_{b\bar{b}}$ tends to zero).

For experiments where a sizeable number of $b\bar{b}$ pairs is produced, one can use the Υ decays to produce HNLs with $M_N \gtrsim 5\text{GeV}$. The number of thus produced HNLs is given by

$$N_{\Upsilon \to N\bar{\nu}} \simeq 10^{-10} N_\Upsilon \times \left(\frac{U^2}{10^{-5}}\right) \quad (3.1.7)$$

where N_Υ is the total number of Υ mesons produced and we have normalized U^2 to the current experimental limit for $M_N > 5$ GeV (c.f. Fig. 3.1). It should be noted that HNLs with the mass of 5 GeV and $U^2 \sim 10^{-5}$ have the decay length $c\tau \sim$ cm.

3.1.1.6 Production from baryons

Semileptonic decays of heavy flavored baryons (Table 3.2) produce HNLs. Baryon number conservation implies that either proton or neutron (or other heavier baryons) must be produced in the heavy baryon decay. This shrinks the kinematic window for the sterile neutrino by about 1 GeV. The corresponding heavy meson decays have an obvious advantage in this respect. Moreover, since both baryons and sterile neutrinos are fermions, only the baryon decays into three and more particles in the final state can yield sterile neutrinos, which further shrinks the sterile neutrino kinematic window with respect to the meson case, where 2-body, purely leptonic decays can produce sterile neutrinos.

Furthermore, lightly-flavored baryons and strange baryons (see Table 3.2) can only produce HNLs in the mass range where the bounds are very strong already (roughly below kaon mass, see FIG. 3.1). Indeed, as weak decays change the strangeness by 1 unit, there the double-strange Ξ-baryons can only decay to Λ or Σ baryons (plus electron or muon and HNL). The maximal mass of the HNL that can be produced in this process is *smaller* than $(M_{\Xi^-} - M_{\Lambda^0}) \simeq 200\,\text{MeV}$. Then, Ω^- baryon decays to $\Xi^0\ell^-N$ with the maximal HNL mass not exceeding $M_{\Omega^-} - M_{\Xi^0} \simeq 350\,\text{MeV}$. Finally, weak decays of Λ or Σ baryons to (p, n) can produce only HNLs lighter than $\sim 250\,\text{MeV}$.

The production of HNL in the decays of charmed and beauty hyperons has been investigated in Ref. [224]; these results have been recently checked in [225]. The number of such baryons is of course strongly suppressed as compared to the number of mesons with the same flavor. At the same time, the masses of HNLs produced in the decay of charmed (beauty) baryons are *below* the threshold of HNL production of the corresponding charmed (beauty) mesons due to the presence of a baryon in the final state. This makes such a production channel strongly subdominant. Dedicated studies for SHiP [221] and at the LHC [225] confirm this conclusion. It should be noted that Refs. [221, 224] use form factors from Ref. [226] which are about 20 years old. A lot of progress has been made since then (see e.g. [227, 228], where some of these form factors were re-estimated and a factor of ~ 2 differences with older estimates were established).

3.1.2 HNL production from tau leptons

At the center-of-mass energies well above the $\bar{c}c$ threshold τ-leptons are copiously produced mostly via $D_s \to \tau + X$ decays. Then HNLs can be produced in τ decays that are important in the case of dominant mixing with τ flavor (which is the one least constrained, see [110, Chapter 4]). The main decay channels of τ are $\tau \to N + h_{P/V}$, $\tau \to N\ell_\alpha\bar{\nu}_\alpha$ and $\tau \to \nu_\tau\ell_\alpha N$, where $\alpha = e, \mu$. Computations of the corresponding decays widths are similar to the processes $N \to \ell_\alpha h_{P/V}$ (c.f. Appendix B.2) and purely leptonic decays of HNL (see Section 3.2.1.1). The results are

$$\Gamma(\tau \to N h_P) = \frac{G_F^2 f_h^2 m_\tau^3}{16\pi} |V_{UD}|^2 |U_\tau|^2 \left[\left(1 - y_N^2\right)^2 - y_h^2 (1 + y_N^2) \right] \sqrt{\lambda(1, y_N^2, y_h^2)} \tag{3.1.8}$$

$$\Gamma(\tau \to N h_V) = \frac{G_F^2 g_h^2 m_\tau^3}{16\pi m_h^2} |V_{UD}|^2 |U_\tau|^2 \left[\left(1 - y_N^2\right)^2 + y_h^2 (1 + y_N^2 - 2y_h^2) \right] \sqrt{\lambda(1, y_N^2, y_h^2)} \tag{3.1.9}$$

$$\begin{aligned}\Gamma(\tau \to N \ell_\alpha \bar{\nu}_\alpha) &= \frac{G_F^2 m_\tau^5}{96\pi^3} |U_\tau|^2 \int\limits_{y_\ell^2}^{(1-y_N)^2} \frac{d\xi}{\xi^3} \left(\xi - y_\ell^2\right)^2 \sqrt{\lambda(1, \xi, y_N^2)} \times \\ &\times \left(\left(\xi + 2y_\ell^2\right) \left[1 - y_N^2\right]^2 + \xi \left(\xi - y_\ell^2\right) \left[1 + y_N^2 - y_\ell^2\right] - \xi y_\ell^4 - 2\xi^3 \right) \\ &\approx \frac{G_F^2 m_\tau^5}{192\pi^3} |U_\tau|^2 \left[1 - 8y_N^2 + 8y_N^6 - y_N^8 - 12 y_N^4 \log(y_N^2)\right], \quad \text{for } y_l \to 0\end{aligned} \tag{3.1.10}$$

$$\begin{aligned}\Gamma(\tau \to \nu_\tau \ell_\alpha N) &= \frac{G_F^2 m_\tau^5}{96\pi^3} |U_\alpha|^2 \int\limits_{(y_\ell + y_N)^2}^{1} \frac{d\xi}{\xi^3} (1 - \xi)^2 \sqrt{\lambda(\xi, y_N^2, y_\ell^2)} \times \\ &\times \left(2\xi^3 + \xi - \xi (1 - \xi) \left[1 - y_N^2 - y_\ell^2\right] - (2 + \xi) \left[y_N^2 - y_\ell^2\right]^2 \right) \approx \\ &\approx \frac{G_F^2 m_\tau^5}{192\pi^3} |U_\alpha|^2 \left[1 - 8y_N^2 + 8y_N^6 - y_N^8 - 12 y_N^4 \log(y_N^2)\right], \quad \text{for } y_l \to 0\end{aligned} \tag{3.1.11}$$

where $y_i = m_i/m_\tau$, V_{UD} is an element of the CKM matrix which corresponds to quark content of the meson h_P; f_h and g_h are pseudoscalar and vector meson decay constants (see Tables C.2 and C.3) and λ is the Källén function [229]:

$$\lambda(a, b, c) = a^2 + b^2 + c^2 - 2ab - 2ac - 2bc \tag{3.1.12}$$

The results of this section fully agree with the literature [218].

3.1.3 HNL production via Drell-Yan and other parton-parton scatterings

The different matrix elements for HNL production in the proton-proton collisions are shown in Fig. 3.7. Here we are limited by the beam energy being not high enough to produce real weak bosons on the target protons. There are three types of processes: Drell-Yan-type process (a), gluon fusion (b) and $W\gamma/g$ fusion (c). Process (b) starts to play an important role for much higher center-of-mass energies [230, 231], processes (a) and (c) should be studied more accurately.

Let us start with the Drell-Yan process (a) in Fig. 3.7. The cross section at the

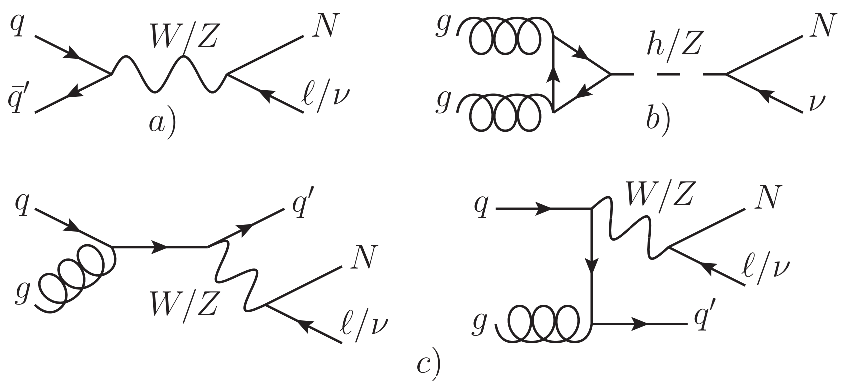

Figure 3.7: HNL production channels: a) Drell-Yan-type process; b) gluon fusion; c) quark-gluon fusion.

parton level is [232, 233]

$$\sigma(\bar{q}q' \to N\ell) = \frac{G_F^2 |V_{qq'}|^2 |U_\ell|^2 s_{\bar{q}q'}}{6 N_c \pi} \left(1 - \frac{3M_N^2}{2 s_{\bar{q}q'}} + \frac{M_N^6}{2 s_{\bar{q}q'}^3}\right), \quad s_{\bar{q}q'} > M_N^2 \tag{3.1.13}$$

where $V_{qq'}$ is an element of the CKM matrix, $N_c = 3$ is a number of colors and the centre-of-mass energy of the system $\bar{q}q'$ is given by

$$s_{\bar{q}q'} = s x_1 x_2 \tag{3.1.14}$$

where x_1 and x_2 are fractions of the total proton's momentum carried by the quark q' and anti-quark $\bar{q}$ respectively. The total cross-section, therefore, is written as

$$\begin{aligned}\sigma(\bar{q}q' \to N\ell) = 2 \sum_{\bar{q},q'} \frac{G_F^2 |V_{qq'}|^2 |U_\ell|^2 s}{6 N_c \pi} \\ \times \int \frac{dx_1}{x_1} x_1^2 f_{\bar{q}}(x_1, s_{\bar{q}q'}) \int \frac{dx_2}{x_2} x_2^2 f_{q'}(x_2, s_{\bar{q}q'}) \left(1 - \frac{3M_N^2}{2 s x_1 x_2} + \frac{M_N^6}{2 s^3 x_1^3 x_2^3}\right) \\ \equiv \frac{G_F^2 |V_{qq'}|^2 |U_\ell|^2 s}{6 N_c \pi} S(\sqrt{s}, M_N)\end{aligned} \tag{3.1.15}$$

where $f_q(x, Q^2)$ is the parton distribution function (PDF). The corresponding integral $S(\sqrt{s}, M_N)$ as a function of M_N and the production probability for this channel are shown in Fig. 3.8. For numerical estimates we have used the LHAPDF package [234] with the CT10NLO PDF set [235].

This can be roughly understood as follows: PDFs peak at $x \ll 1$ (see Fig. 3.9) and therefore the probability that the center-of-mass energy of a parton pair exceeds the HNL mass, $\sqrt{s_{parton}} \gg M_N$, is small. On the other hand, the probability of a flavored meson to decay into an HNL (for $|U|^2 \sim 1$) is of the order of few % and

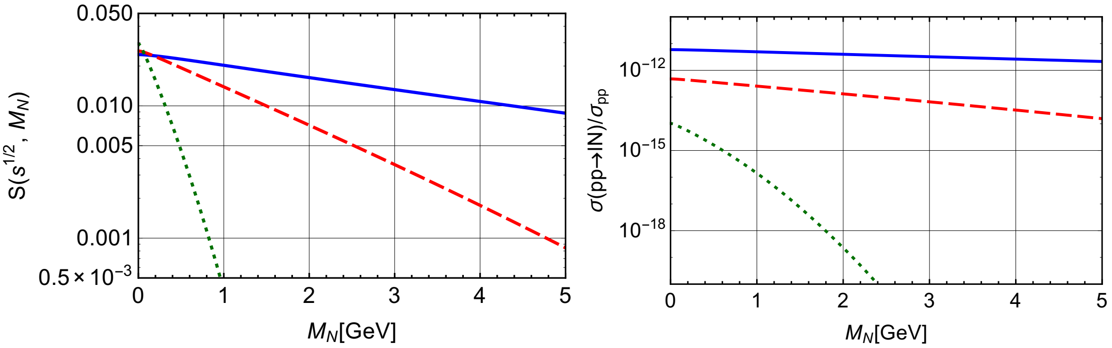

Figure 3.8: Integral (3.1.15) as a function of HNL's mass, neglecting lepton mass (left panel) and probability of HNL production in p-p collision for $|U_\ell| = 1$ (right panel) for $\sqrt{s} = 100$ GeV (blue line), $\sqrt{s} = 28$ GeV (red dashed line) and $\sqrt{s} = 4$ GeV (green dotted line). The suppression of the integral as compared to $M_N = 0$ case is due to PDFs being small at $x \sim 1$ and condition $x_1 x_2 s > M_N^2$. Total p-p cross-section is taken from [222].

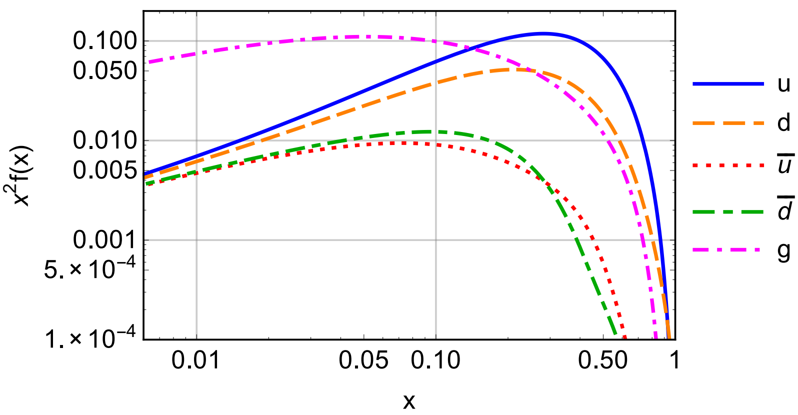

Figure 3.9: Combination $x^2 f(x)$ used in Eq. (3.1.15) for quark and gluon PDFs (for $\sqrt{s} \sim 30$ GeV). The functions peak at small values of x and therefore the probability of the center-of-mass energy of the parton pair close to $\sqrt{s}$ is small.

therefore "wins" over the direct production, especially at the fixed-target experiments where the beam energies do not exceed hundreds of GeV. In case of the quark-gluon initial state (process (c) in Fig. 3.7) similar considerations also work and the resulting cross-section is also small, with an additional suppression due to the 3-body final state. *We see that the direct production channel is strongly suppressed in comparison with the production from mesons for HNLs with masses $M_N \lesssim 5\,\mathrm{GeV}$.*

3.1.4 Coherent proton-nucleus scattering

The coherent scattering of a proton on the nuclei as a whole could be an effective way of producing new particles in fixed-target experiments. There are two reasons for this. Firstly, parton scattering in the electromagnetic field of the nuclei is proportional to

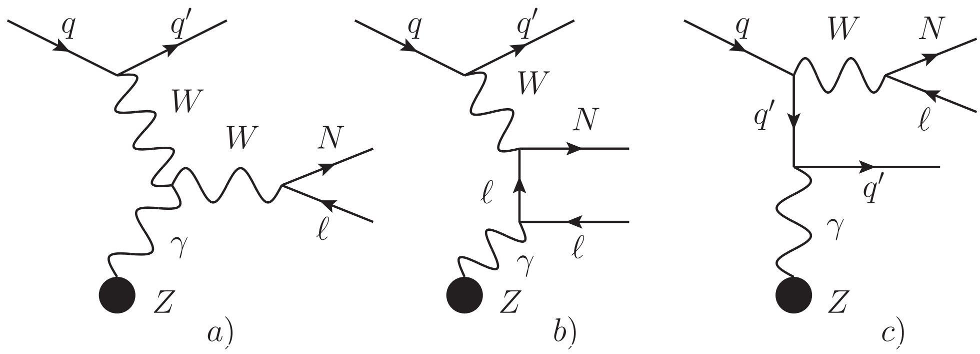

Figure 3.10: Possible Feynman diagrams for the HNL production in the proton coherent scattering off the nuclei.

Z^2 (where Z is the nuclei charge) which can reach a factor 10^3 enhancement for heavy nuclei. Secondly, the center of mass energy of the proton-nucleus system is higher than for the proton-proton scattering. The coherent production of the HNLs will be discussed in the forthcoming paper [236]. Here we announce the main result: the coherent HNL production channel is subdominant to the meson decay for all HNL masses and mixing angles (for HNL masses below 5 GeV). In case of SHiP one expects less than 1 HNL *produced* via coherent scattering for 10^{20} PoT.

3.1.5 Summary

In summary, production of HNL in proton fixed-target experiments occurs predominantly via (semi)leptonic decays of the lightest c- and b- mesons (Figs. 3.4, 3.5). The production from heavier mesons is suppressed by the strong force-mediated SM decays, while production from baryons is kinematically suppressed. Other production channels are subdominant for all masses $0.5\,\text{GeV} \leq M_N \leq 5\,\text{GeV}$ as discussed in Sections 3.1.3–3.1.4.

3.2 HNL decay modes

All HNL decays are mediated by the charged or the neutral current interactions. In this Section, we systematically revisit the most relevant decay channels. Most of the results for sufficiently light HNLs exist in the literature [217, 218, 220, 237–239]. For a few modes, there are discrepancies by factors of few between different works, we comment on these discrepancies in due course.

All the results presented below *do not take into account charge conjugated channels* which are possible for the Majorana HNL; to account for the Majorana nature one should multiply all the decay widths by 2. The branching ratios are the same for Majorana case and for the case considered here.

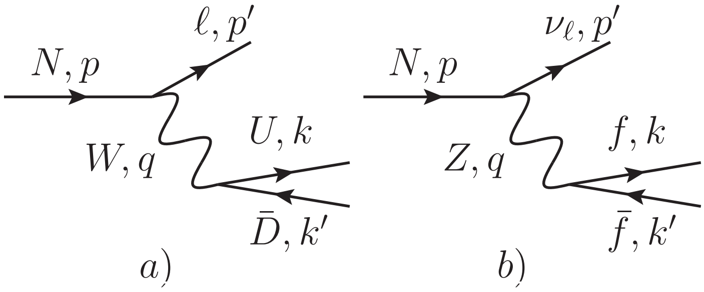

Figure 3.11: Diagram for the HNL decays mediated by charged (a) and neutral (b) currents.

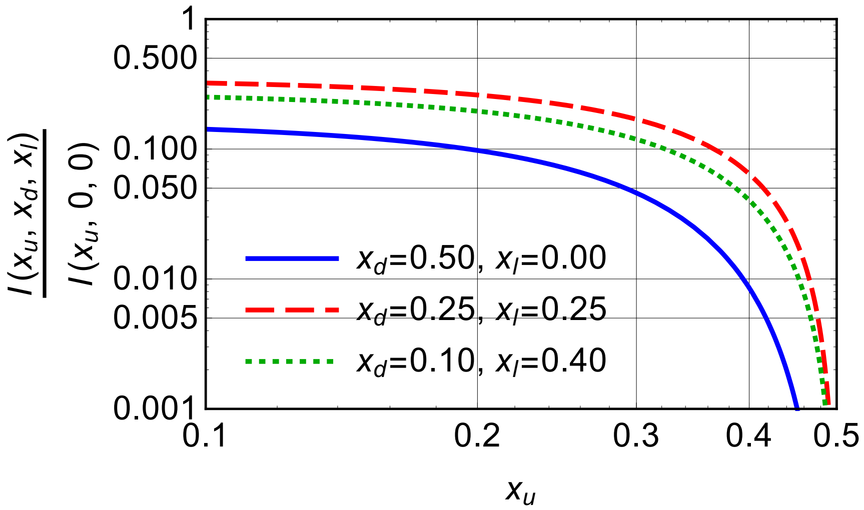

Figure 3.12: Function $I(x_u, x_d, x_l)/I(x_u, 0, 0)$ for several choices of x_d and x_l (see Eq. (3.2.2) for $I(x_u, x_d, x_l)$ definition).

3.2.1 3-body basic channels

Two basic diagrams, presented in the Fig. 3.11, contribute to all decays. For the charged current-mediated decay (Fig. 3.11(a)) the final particles (U, D) could be either a lepton pair $(\nu_\alpha, \ell_\alpha)$ or a pair of up and down quarks (u_i, d_j). For the neutral current-mediated decay f stands for any fermion. The tree-level decay width into free quarks, while unphysical by itself for the interesting mass range, is important in estimates of the full hadronic width at $M_N \gg \Lambda_{\mathrm{QCD}}$, see Section 3.2.2.2 below.

For the decays $N \to \nu_\alpha \ell_\alpha^- \ell_\alpha^+$ and $N \to \nu_\alpha \nu_\alpha \bar{\nu}_\alpha$ both diagrams contribute, which leads to the interference (see Section 3.2.1.2).

3.2.1.1 Charged current-mediated decays

The general formula for the charged current-mediated processes $N \to \ell_\alpha^- \nu_\beta \ell_\beta^+$, $\alpha \neq \beta$, and $N \to \ell_\alpha u_i \bar{d}_j$ is [237–240]

$$\Gamma(N \to \ell_\alpha^- U \bar{D}) = N_W \frac{G_F^2 M_N^5}{192\pi^3} |U_\alpha|^2 I(x_u, x_d, x_l) \tag{3.2.1}$$

where $x_l = \dfrac{m_{\ell_\alpha}}{M_N}$, $x_u = \dfrac{m_U}{M_N}$, $x_d = \dfrac{m_D}{M_N}$. The factor $N_W = 1$ for the case of the final leptons and $N_W = N_c |V_{ij}|^2$ in the case of the final quarks, where $N_c = 3$ is the number of colors, and V_{ij} is the corresponding matrix element of the CKM matrix. The function $I(x_u, x_d, x_l)$ that describes corrections due to finite masses of final state fermions is given by

$$I(x_u, x_d, x_l) \equiv 12 \int\limits_{(x_d+x_l)^2}^{(1-x_u)^2} \frac{dx}{x} \left(x - x_l^2 - x_d^2\right) \left(1 + x_u^2 - x\right) \sqrt{\lambda(x, x_l^2, x_d^2)\lambda(1, x, x_u^2)}, \tag{3.2.2}$$

where $\lambda(a, b, c)$ is given by Eq. (3.1.12).

Several properties of the function (3.2.2):

1. $I(0, 0, 0) = 1$
2. Function $I(a, b, c)$ is symmetric under *any* permutation of its arguments a, b, c.[4]
3. In the case of mass hierarchy $m_a, m_b \ll m_c$ (where a, b, c are leptons and/or quarks in some order) one can use an approximate result

$$I(x, 0, 0) = (1 - 8x^2 + 8x^6 - x^8 - 12x^4 \log x^2) \tag{3.2.3}$$

   where $x = \dfrac{m_c}{M_N}$.
4. The ratio $I(x_u, x_d, x_l)/I(x_u, 0, 0)$ for several choices of x_d, x_l is plotted in Fig. 3.12. It decreases with each argument.

3.2.1.2 Decays mediated by neutral current interaction and the interference case

Decay width for neutral current-mediated decay $N \to \nu_\alpha f \bar{f}$ depends on the type of the final fermion. For charged lepton pair $l_\beta \bar{l}_\beta$ the results are different for the case $\alpha \neq \beta$ and $\alpha = \beta$, because of the existence of the charge current mediated diagrams

[4] This property is non-obvious but can be verified by the direct computation.

in the latter case. Nevertheless, the decay width can be written in a unified way,

$$\Gamma(N \to \nu_\alpha f \bar{f}) = N_Z \frac{G_F^2 M_N^5}{192\pi^3} \cdot |U_\alpha|^2 \cdot \left[C_1^f \left((1 - 14x^2 - 2x^4 - 12x^6)\sqrt{1-4x^2} + \right.\right.$$
$$\left. + 12x^4(x^4 - 1)L(x) \right) + 4C_2^f \left(x^2(2 + 10x^2 - 12x^4)\sqrt{1-4x^2} + \right.$$
$$\left.\left. + 6x^4(1 - 2x^2 + 2x^4)L(x) \right) \right], \tag{3.2.4}$$

where $x = \dfrac{m_f}{M_N}$, $L(x) = \log\left[\dfrac{1 - 3x^2 - (1 - x^2)\sqrt{1-4x^2}}{x^2(1 + \sqrt{1-4x^2})}\right]$ and $N_Z = 1$ for the case of leptons in the final state or $N_Z = N_c$ for the case of quarks. The values of C_1^f and C_2^f are given in the Table 3.3. This result agrees with [218, 238, 239].

f	C_1^f	C_2^f
$u,\ c,\ t$	$\frac{1}{4}\left(1 - \frac{8}{3}\sin^2\theta_W + \frac{32}{9}\sin^4\theta_W\right)$	$\frac{1}{3}\sin^2\theta_W\left(\frac{4}{3}\sin^2\theta_W - 1\right)$
$d,\ s,\ b$	$\frac{1}{4}\left(1 - \frac{4}{3}\sin^2\theta_W + \frac{8}{9}\sin^4\theta_W\right)$	$\frac{1}{6}\sin^2\theta_W\left(\frac{2}{3}\sin^2\theta_W - 1\right)$
$\ell_\beta,\ \beta \neq \alpha$	$\frac{1}{4}\left(1 - 4\sin^2\theta_W + 8\sin^4\theta_W\right)$	$\frac{1}{2}\sin^2\theta_W\left(2\sin^2\theta_W - 1\right)$
$\ell_\beta,\ \beta = \alpha$	$\frac{1}{4}\left(1 + 4\sin^2\theta_W + 8\sin^4\theta_W\right)$	$\frac{1}{2}\sin^2\theta_W\left(2\sin^2\theta_W + 1\right)$

Table 3.3: Coefficients C_1 and C_2 for the neutral current-mediated decay width.

In the case of pure neutrino final state only neutral currents contribute and the decays width reads

$$\Gamma(N \to \nu_\alpha \nu_\beta \bar{\nu}_\beta) = (1 + \delta_{\alpha\beta}) \frac{G_F^2 M_N^5}{768\pi^3} |U_\alpha|^2. \tag{3.2.5}$$

3.2.2 Decay into hadrons

In this Section, we consider hadronic final states for M_N both below and above Λ_{QCD} scale and discuss the range of validity of our results.

3.2.2.1 A single meson in the final state

At $M_N \lesssim \Lambda_{\text{QCD}}$ the quark pair predominantly binds into a single meson. There are both charged and neutral current-mediated processes with a meson in the final state: $N \to \ell_\alpha h^+_{P/V}$ and $N \to \nu_\alpha h^0_{P/V}$, where h^+_P (h^0_P) are charged (neutral) pseudoscalar mesons and h^+_V (h^0_V) are charged (neutral) vector mesons. In formulas below $x_h \equiv m_h/M_N$, $x_\ell = m_\ell/M_N$, f_h and g_h are the corresponding meson decay constants (see Appendix C.1), θ_W is a Weinberg angle and the function λ is given by eq. (3.1.12). The details of the calculations are given in the Appendix B.2.

The decay width to the charged pseudo-scalar mesons $(\pi^\pm, K^\pm, D^\pm, D_s, B^\pm, B_c)$ is given by

$$\Gamma(N \to \ell_\alpha^- h_P^+) = \frac{G_F^2 f_h^2 |V_{UD}|^2 |U_\alpha|^2 M_N^3}{16\pi} \left[\left(1 - x_\ell^2\right)^2 - x_h^2(1 + x_\ell^2)\right] \sqrt{\lambda(1, x_h^2, x_\ell^2)}, \tag{3.2.6}$$

in full agreement with the literature [218, 238, 239].

The decay width to the pseudo-scalar neutral meson $(\pi^0, \eta, \eta', \eta_c)$ is given by

$$\Gamma(N \to \nu_\alpha h_P^0) = \frac{G_F^2 f_h^2 M_N^3}{32\pi} |U_\alpha|^2 \left(1 - x_h^2\right)^2 \tag{3.2.7}$$

Our answer agrees with [218], but is twice larger than [238, 239]. The source of the difference is unknown.[5]

The HNL decay width into charged vector mesons ($\rho^\pm$, $a_1^\pm$, $D^{\pm *}$, $D_s^{\pm *}$) is given by

$$\Gamma(N \to \ell_\alpha^- h_V^+) = \frac{G_F^2 g_h^2 |V_{UD}|^2 |U_\alpha|^2 M_N^3}{16\pi m_h^2} \left(\left(1 - x_\ell^2\right)^2 + x_h^2 \left(1 + x_\ell^2\right) - 2x_h^4\right) \sqrt{\lambda(1, x_h^2, x_\ell^2)} \tag{3.2.8}$$

that agrees with the literature [218, 238, 239].

However, there is a disagreement regarding the numerical value of the meson constant g_ρ between [218] and [238, 239]. We extract the value of this constant from the decay $\tau \to \nu_\tau \rho$ and obtain the result that numerically agrees with the latter works, see discussion in Appendix C.1.3.

For the decay into neutral vector meson (ρ^0, a_1^0, ω, ϕ, J/ψ) we found that the result depends on the quark content of meson. To take it into account we introduce dimensionless κ_h factor to the meson decay constant (B.2.6). The decay width is given by

$$\Gamma(N \to \nu_\alpha h_V^0) = \frac{G_F^2 \kappa_h^2 g_\rho^2 |U_\alpha|^2 M_N^3}{32\pi m_h^2} \left(1 + 2x_h^2\right) \left(1 - x_h^2\right)^2. \tag{3.2.9}$$

Our result for ρ^0 and results in [218] and [238] are all different. The source of the difference is unknown. For decays into ω, ϕ and J/ψ mesons we agree with [238]. The result for the a_1^0 meson appears for the first time.[6]

The branching ratios for the one-meson and lepton channels below 1 GeV are given on the left panel of Fig. 3.13.

[5] This cannot be due to the Majorana or Dirac nature of HNL, because the same discrepancy would then appear in Eq. (3.2.6).

[6] Refs. [238, 239] quote also 2-body decays $N \to \nu_\alpha h_V^0$, $h_V^0 = K^{*0}, \bar{K}^{*0}, D^{*0}, \bar{D}^{*0}$, with the rate given by (3.2.9) (with a different κ). This is not justified since the weak neutral current does not couple to the corresponding vector meson h_V^0 at tree level.

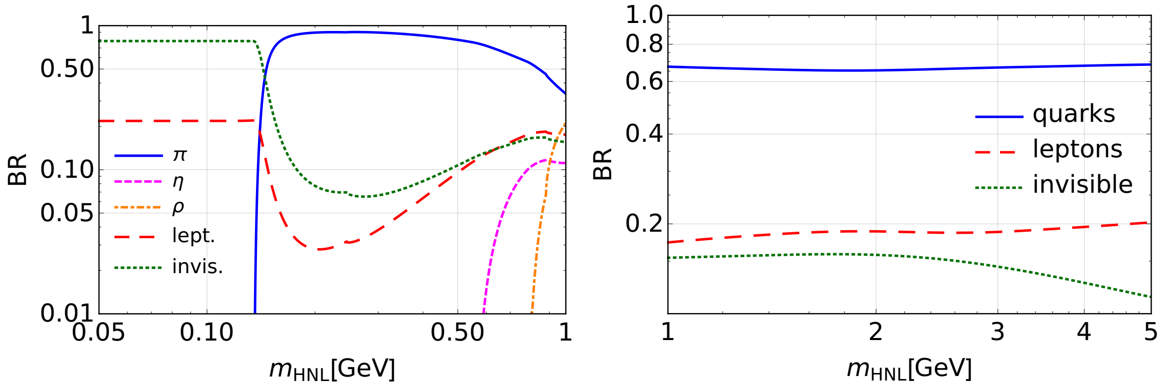

Figure 3.13: The branching ratios of the HNL for the mixing ratio $U_e : U_\mu : U_\tau = 1 : 1 : 1$. *Left panel:* region of masses below 1 GeV; *Right panel:* region of masses above 1 GeV, for quarks the QCD corrections (3.2.10), (3.2.11) are taken into account.

3.2.2.2 Full hadronic width vs. decay into single meson final state

Decays into multi-hadron final states become kinematically accessible as soon as $M_N > 2m_\pi$. To estimate their branching fractions and their contribution to the total decay width, we can compute the total hadronic decay width of HNLs, $\Gamma_{\rm had}$ and compare it with the combined width of all single-meson states, $\Gamma_{1\,\rm meson}$. The total hadronic decay width can be estimated via decay width into quarks (Sections 3.2.1.1–3.2.1.2) times the additional loop corrections.

The QCD loop corrections to the tree-level decay into quarks have been estimated in the case of τ lepton hadronic decays. In this case, the tree-level computation of the τ decay to two quarks plus neutrino underestimates the full hadronic decay width by 20% [241–243]. The loop corrections, $\Delta_{\rm QCD}$, defined via

$$1 + \Delta_{\rm QCD} \equiv \frac{\Gamma(\tau \to \nu_\tau + \text{hadrons})}{\Gamma_{\rm tree}(\tau \to \nu_\tau \bar{u} q)} \tag{3.2.10}$$

have been computed up to three loops [243] and is given by:

$$\Delta_{\rm QCD} = \frac{\alpha_s}{\pi} + 5.2\frac{\alpha_s^2}{\pi^2} + 26.4\frac{\alpha_s^3}{\pi^3}, \tag{3.2.11}$$

where $\alpha_s = \alpha_s(m_\tau)$.[7] We use (3.2.11) with $\alpha_s = \alpha_s(M_N)$ as an estimation for the QCD correction for the HNL decay, for both charged and neutral current processes. We expect therefore that QCD correction to the HNL decay width into quarks is smaller than 30% for $M_N \gtrsim 1$ GeV (Fig. 3.14).

Full hadronic decay width dominates the HNL lifetime for masses $M_N \gtrsim 1$ GeV (see Fig. 3.13). The latter is important to define the upper bound of sensitivity

[7] Numerically this gives for the τ-lepton $\Delta_{\rm QCD} \approx 0.18$, which is within a few % of the experimental value $\Delta_{\rm Exp} = 0.21$. The extra difference comes from the QED corrections.

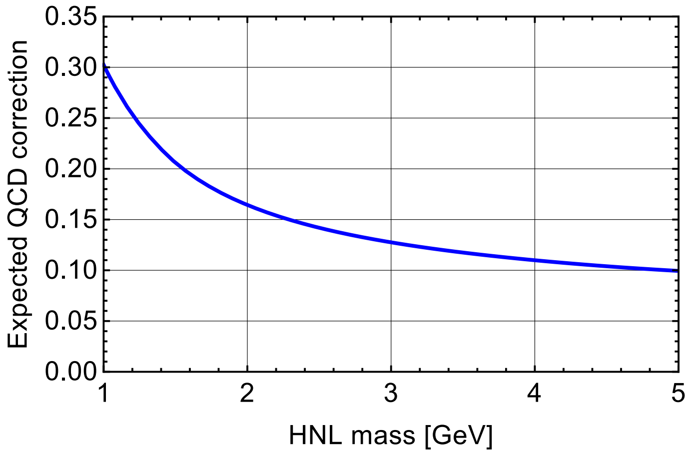

Figure 3.14: The estimate of the QCD corrections for the HNL decay into quark pairs, using the three-loop formula (3.2.11) for τ-lepton.

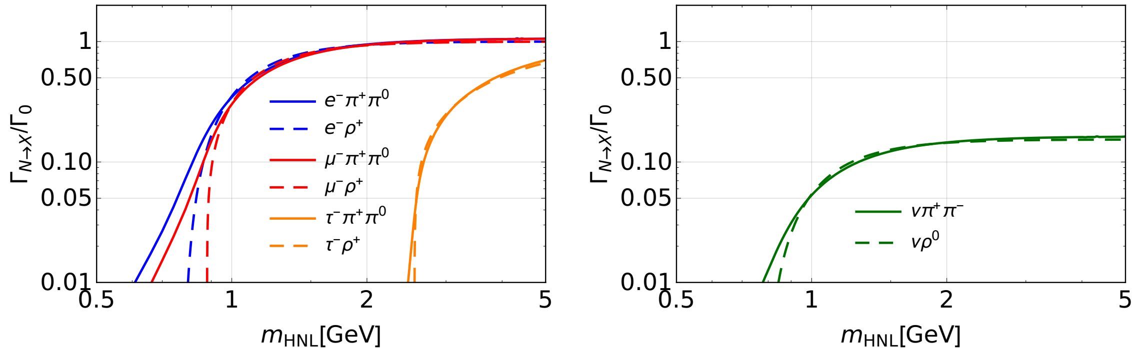

Figure 3.15: *Left panel:* Decay widths of charged current channels with ρ or 2π divided by $\Gamma_0 = \frac{1}{16\pi} G_F^2 \frac{g_\rho^2}{m_\rho^2} |V_{ud}|^2 |U_\alpha|^2 M_N^3$, which is the prefactor in Eq. (3.2.8). *Right panel:* The same for neutral current channels.

for the experiments like SHiP or MATHUSLA (see Fig. 3.1). This upper bound is defined by the requirements that HNLs can reach the detector.

3.2.2.3 Multi-meson final states

When discussing "single-meson channels" above, we have also included there decays with the ρ-meson. By doing so, we have essentially incorporated all the two-pion decays $N \to \pi^+\pi^0\ell^-$ for $M_N > m_\rho$. Indeed, we have verified by direct computation of $N \to \pi^+\pi^0\ell^-$ that they coincide with $N \to \rho^+\ell^-$ for all relevant masses (Fig. 3.15). Of course, the decay channel to two pions is also open for $2m_\pi < M_N < m_\rho$, but its contribution there is completely negligible and we ignore it in what follows.

Figs. 3.13 and 3.16 demonstrate that one-meson channels are definitely enough for all the hadronic modes if sterile neutrino mass does not exceed 1 GeV. The ratio between the combined decay width into single-meson final states ($\pi^\pm$, π^0, η, η', $\rho^\pm$,

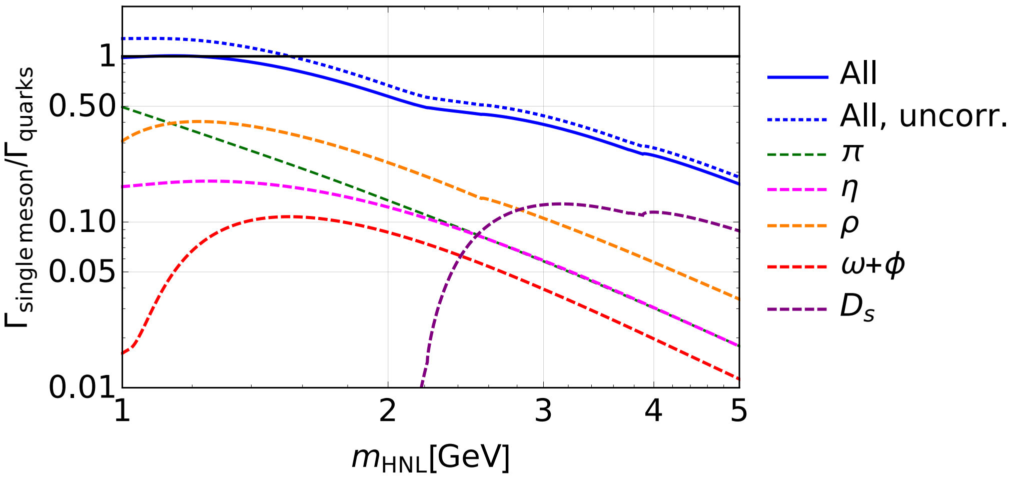

Figure 3.16: HNL decay widths into all relevant single meson channels, divided by the total decay width into quarks with QCD corrections, estimated as in (3.2.11) (all dashed lines). The blue solid line is the sum of all mesons divided by decay width into quarks with QCD corrections, the blue dotted line is the same but without QCD corrections.

3-body decays
$N \to \ell_\alpha^- \pi^+ \pi^0$
$N \to \nu_\alpha \pi^+ \pi^-$
$N \to \nu_\alpha \pi^0 \pi^0$
$N \to \ell_\alpha^- K^+ \bar{K}^0$
$N \to \nu_\alpha K^+ K^-$
$N \to \nu_\alpha K^0 \bar{K}^0$
$N \to \ell_\alpha^- K^+ \pi^0$
$N \to \ell_\alpha^- K^0 \pi^+$

4-body decays
$N \to \nu_\alpha (3\pi)^0$
$N \to \ell_\alpha^- (3\pi)^+$
$N \to \nu_\alpha (2\pi K)^0$
$N \to \ell_\alpha^- (2\pi K)^+$
$N \to \nu_\alpha (2K\pi)^0$
$N \to \ell_\alpha^- (2K\pi)^+$
$N \to \ell_\alpha^- (3K)^+$
$N \to \nu_\alpha (3K)^0$

Branching ratios $\tau^- \to \nu_\tau + X^-$	[%]
$\tau \to \nu_\tau + \pi^-$	10.8
$\tau \to \nu_\tau + \pi^- \pi^0$	25.5
$\tau \to \nu_\tau + \pi^0 \pi^- \pi^0$	9.2
$\tau \to \nu_\tau + \pi^- \pi^+ \pi^-$	9.0
$\tau \to \nu_\tau + \pi^- \pi^+ \pi^- \pi^0$	4.64
$\tau \to \nu_\tau + \pi^- \pi^0 \pi^0 \pi^0$	1.04
$\tau \to \nu_\tau + 5\pi$	$\mathcal{O}(1)$
$\tau \to \nu_\tau + K^-$ or $K^- \pi^0$	$\mathcal{O}(1)$
$\tau \to \nu_\tau + K^- K^0$	$\mathcal{O}(0.1)$
$\tau \to \nu_\tau + K^- K^0 \pi^0$	$\mathcal{O}(0.1)$

Table 3.4: Possible multi-meson decay channels of HNLs with $M_N > 2m_\pi$ threshold. Right panel shows branching ratios of hadronic decays of the τ-lepton and demonstrates the relative importance of various hadronic 2-, 3-, 4- and 5-body channels.

ρ^0, ω+ϕ, D_s) and into quarks is shown in Fig. 3.16.[8] One sees that the decay width into quarks is larger for $M_N \gtrsim 2$ GeV, which means that multi-meson final states are important in this region.

The main expected 3- and 4-body decay channels of HNLs are presented in Table 3.4. We also add information about multi-meson decays of τ because they give us information about decay through charged current of the HNL of the same mass as

[8]We ignore CKM-suppressed decays into kaons as well as decays to heavy flavor meson (D,B).

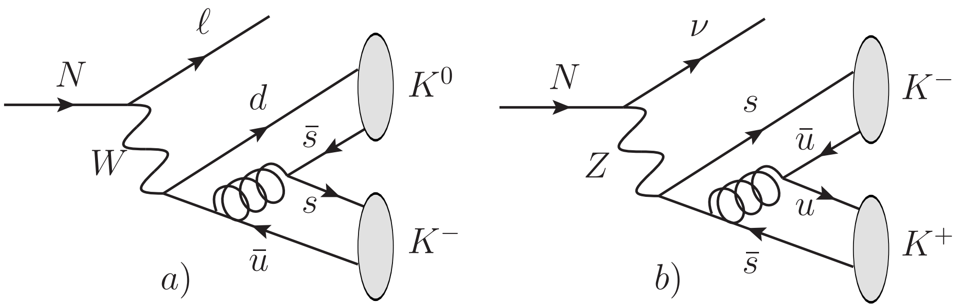

Figure 3.17: HNL decays into 2 kaons through charged (a) and neutral (b) currents.

τ-lepton. The main difference between HNL and τ-lepton comes from the possibility of the HNL decay through the neutral current, which we discuss below.

The main hadronic channels of the τ are n-pions channels. Decay channel into 2 pions is the most probable, but there is a large contribution from the 3-pion channels and still appreciable contribution from the 4-pion ones. For bigger masses the contribution from the channels with higher multiplicity become more important as the Fig. 3.16 demonstrates.

The decay into kaons is suppressed for the τ-lepton. For some channels like $\tau \to \nu_\tau K$ or $\tau \to \nu_\tau K\pi$ this suppression comes from the Cabibbo angle between s and u quarks. The same argument holds for HNL decays into a lepton and D meson, but not in D_s. The decays like $\tau \to \nu_\tau K^- K^0$ are not suppressed by the CKM matrix and still are small. We think that this is because for such decays the probability of the QCD string fragmentation into strange quarks is much smaller than into u and d quarks for the given τ-lepton mass (see diagram (a) in Fig. 3.17). At higher masses, the probability of such fragmentation should be higher, but still too small to take it into account. On the other hand, the HNL decay into two kaons can give a noticeable contribution, because of the existence of the neutral current decay (see diagram (b) in Fig. 3.17), for which the previous arguments do not apply.